Pergamon

0301-9322(95)00037-2

Int. J. Multiphase Flow Vol. 21, No. 6, pp. 1229–1236, 1995

0301-9322/95 $9.50 + 0.00

FLOW REGIME DIAGRAMS FOR GAS–SOLID FLUIDIZATION AND UPWARD TRANSPORT

H. T. BI and J. R. GRACE†

Department of Chemical Engineering, University of British Columbia, Vancouver, Canada V6T 1Z4

(Received 5 January 1995; in revised form 26 April 1995)

Abstract—Flow regime maps are presented for gas–solids fluidized beds and gas–solids upward transport lines. For conventional gas–solids fluidization, the flow regimes include the fixed bed, bubbling fluidization, slugging fluidization and turbulent fluidization. For gas–solids vertical transport operation, solids flux must be incorporated in the flow regime diagrams. The flow regimes then include dilute-phase transport, fast fluidization or turbulent flow, slug/bubbly flow, bubble-free dense-phase flow and packed bed flow. In practical circulating fluidized beds and transport risers, operation below the fast fluidization regime is commonly impossible due to equipment limitations. Practical flow regime maps are proposed with the flow regimes, including homogeneous dilute-phase flow, core–annular dilute-phase flow (where there are appreciable lateral gradients but small axial gradients) and fast fluidization (where there are both lateral and axial gradients). The boundary between fast fluidization and dilute-phase pneumatic transport is set by the type A choking velocity, at which the uniform suspension collapses and particles start to accumulate in the bottom region of the transport line, while the mechanism of transition from fast fluidization to dense-phase flow depends on the column and particle diameters.

Key Words: gas–solid fluidization, vertical pneumatic transport, flow regime diagrams

1. INTRODUCTION

Various attempts have been made to plot flow regime maps for gas–solid suspensions. In an early study, Zenz (1949) proposed a flow diagram in which both dense fluidization and co-current pneumatic flow regimes are indicated, but the "turbulent" region around which both slugging and choking are present was not delineated. A similar flow regime map was proposed by Yerushalmi *et al.* (1976, 1978) in which bed voidage was plotted against superficial gas velocity to show the transitions among the packed bed, bubbling bed, turbulent fluidization and fast fluidization regimes. The regime map developed by Li & Kwauk (1980) also plots voidage against superficial gas velocity. Squires *et al.* (1985) expanded such a map to include the pneumatic transport regime and choking points, and this was further modified by Rhodes (1987). The transition from low velocity to high velocity fluidization is, however, still poorly characterized. Grace (1986) extended and modified the approach of Reh (1971) to propose a unified regime diagram based on literature data to show the operating ranges of conventional fluidized beds, spouted beds, circulating beds and transport systems. The transition from low-velocity to high-velocity fluidization was not clearly delineated, although some data available at that time were plotted to indicate the onset of turbulent fluidization.

Following another approach, Leung (1980), Klinzing (1981) and Yang (1983) proposed flow regime maps of gas–solids transport in which gas velocity was plotted against solids flux, with gas–solid transport divided into dense-phase flow and dilute-phase flow regimes. The termination of pneumatic transport to dense-phase fluidization was again unclear. Takeuchi *et al.* (1986) proposed a flow map based on their experimental findings to define the boundaries of fast fluidization. This flow regime map was modified by Bi & Fan (1991) to include the transition from heterogenous dilute flow to the homogeneous dilute flow regime. Hirama *et al.* (1992), on the other hand, tried to extend such a diagram to the transition from high-velocity to low-velocity fluidization, but the transition was again not fully defined.

†To whom correspondence should be addressed.

In this paper, unified flow regime diagrams are proposed based on previous and recent experimental findings from this research group (Grace 1986; Bi *et al.* 1993, 1995; Bi & Grace 1994, 1995) to show the relationship between flow regimes for both gas–solid fluidization and co-current upward transport.

2. FLOW REGIMES IN BATCH-OPERATED GAS–SOLID FLUIDIZED BEDS

In a gas–solid fluidized bed, it has long been understood that fixed bed flow transforms to fluidized bed flow at the minimum fluidization velocity, U_{mf}. For fine particle systems, bubbles appear at the minimum bubbling velocity, U_{mb}, while slugs start to form at the minimum slugging velocity, U_{ms}. The transition to the turbulent fluidization regime is generally assumed to occur when the superficial velocity, U, reaches U_c, the superficial velocity at which the standard deviation of pressure fluctuations passes through a maximum. The termination of batch operation of fluidized beds is marked by significant entrainment of bed particles beyond U_{se} where particles can no longer be maintained in the column unless entrained particles are captured and returned to the bed efficiently. Such a flow transition process is depicted in figure 1. For large column diameter, D, or small particle diameter, d_p, the slugging regime may be by-passed altogether. Only small transient voids appear in the turbulent regime between U_c and U_{se}.

A flow regime diagram consistent with the above picture, for cases where the overflow is small enough that the inventory of the column is constant or nearly so, is shown in figure 2. In this diagram, the dimensionless parameters U^* ($=\mathrm{Re}/\mathrm{Ar}^{1/3}$) and d_p^* ($=\mathrm{Ar}^{1/3}$) suggested by Grace (1986) are used as axes, where $\mathrm{Re}=\rho_G U d_p/\mu_G$, and $\mathrm{Ar}=\rho_G(\rho_p-\rho_G)\boldsymbol{g}d_p^3/\mu_G$ are the Reynolds number and Archimedes number, respectively, with ρ_G and ρ_p being the gas and particle density, μ_G the gas viscosity and $\boldsymbol{g}$ the acceleration of gravity. The equation of Grace (1982), modified from the Wen & Yu correlation (1966), is chosen for the calculation of U_{mf},

$$\mathrm{Re}_{mf}=\sqrt{27.2^2+0.0408\,\mathrm{Ar}}-27.2 \qquad [1]$$

U_c, corresponding to the point where the standard deviation of differential pressure fluctuations reaches a maximum, is calculated (Bi & Grace 1994) by

$$\mathrm{Re}_c=1.24\,\mathrm{Ar}^{0.45} \quad (2<\mathrm{Ar}<1\times10^8) \qquad [2]$$

The critical velocity U_{se} is defined as the point where the solids begin to be entrained significantly (Bi *et al.* 1995), setting an upper limit on conventional fluidized bed operation. The U_{se} line in figure 2 is calculated (Bi *et al.* 1995) by

$$\mathrm{Re}_{se}=1.53\,\mathrm{Ar}^{0.50} \quad (2<\mathrm{Ar}<4\times10^6) \qquad [3]$$

Since the transition velocity U_{ms} depends on the column diameter, not included in the dimensionless co-ordinates, U_{ms} cannot be plotted on this diagram. For group A particles, the minimum bubbling velocity can be estimated by the Geldart & Abrahamsen (1978) dimensional correlation,

$$U_{mb}=33d_p\left(\frac{\rho_G}{\mu_G}\right)^{0.1} \qquad [4]$$

which again cannot be included on the diagram.

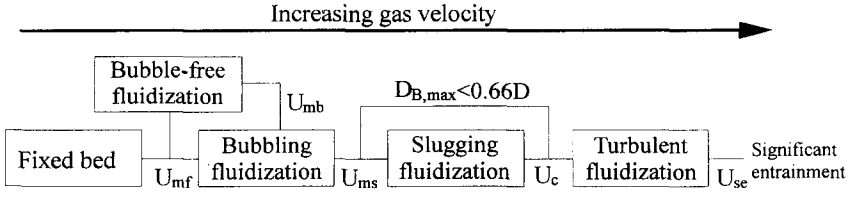

Figure 1. Flow chart showing regime transitions in gas–solid fluidized beds with little or no overflow of solids. $D_{B,max}$ = maximum stable bubble size.

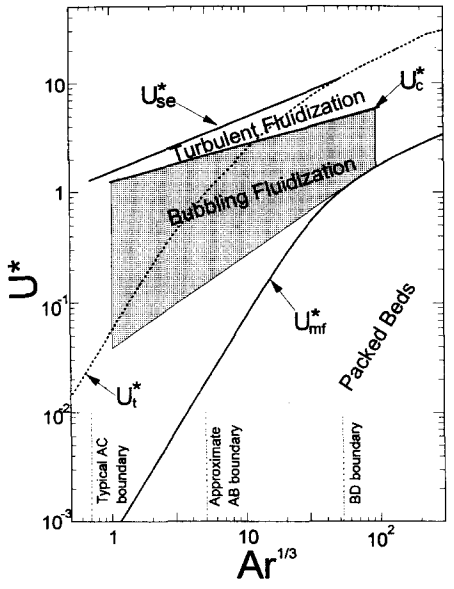

Figure 2. Flow regime map for gas–solids fluidization. Heavy lines indicate transition velocities, while the shaded region bounded by thin lines is the typical operating range of bubbling fluidized beds. Ar = Archimedes number; U_t = terminal velocity of single particles.

3. FLOW PATTERNS IN GAS–SOLID VERTICAL TRANSPORT LINES

A gas–liquid column can be operated under continuous conditions in which liquid is continuously fed to the bottom and overflows from the top. In a gas–solid system, such a transport operation can also be achieved if both gas and solids are supplied at sufficient rates to the bottom of the column, with gas and solids also leaving continuously at the top. Ideally, the flow patterns of the transport line are completely determined by the relative velocity between the gas and particle phase (i.e. by the relative velocity) rather than the superficial gas velocity. Analogous to gas–liquid upward transport, the flow patterns are depicted in figure 3. At a fixed solids flux, G_s, a transport line may experience bubbly flow, slug flow and turbulent flow or fast fluidization before achieving pneumatic transport. A bubble-free dense-phase flow regime may also exist for group A particles. The slug flow regime may again be by-passed for large diameter columns.

In solid transport systems, the transition velocity depends on the relative velocity between the two phases. Ideally, the minimum fluidization velocity, V_{mf}, can be estimated by

$$V_{mf} = U_{mf} + \frac{G_s \epsilon_{mf}}{\rho_p (1 - \epsilon_{mf})} \quad [5]$$

where ϵ_{mf} is the bed voidage at minimum fluidization. Similarly, the minimum bubbling velocity can be predicted by

$$V_{mb} = U_{mb} + \frac{G_s \epsilon_{mb}}{\rho_p (1 - \epsilon_{mb})} \quad [6]$$

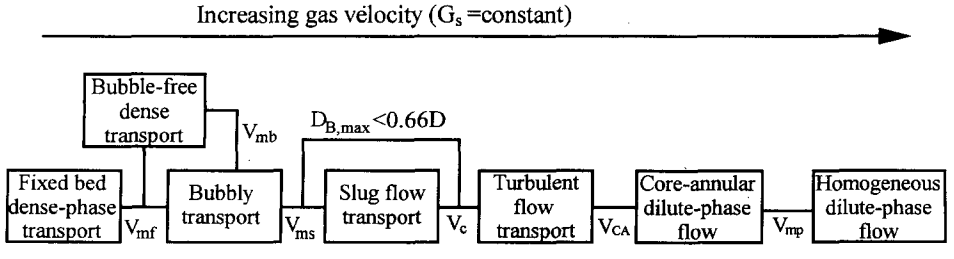

Figure 3. Flow chart showing regime transitions in gas–solids upward transport lines for constant solids flux. V_{mf}, V_{mb}, V_{ms}, V_c, V_{CA} and V_{mp} are defined by [5]–[7], [10], [11] and [16].

where U_{mb} can be calculated from [4] and ϵ_{mb} is the voidage at minimum bubbling. The velocity V_c which marks the onset of fast fluidization or turbulent flow can be estimated by

$$V_c = U_c + \frac{G_s \epsilon_c}{\rho_p (1 - \epsilon_c)} \quad [7]$$

where ϵ_c, the voidage at the transition point, is approximately 0.65 and can be estimated (Bi & Grace 1994) by

$$\epsilon_c = \epsilon_{Bc} + (1 - \epsilon_{Bc})\epsilon_{mf} \quad [8]$$

with the bubble phase volume fraction at this point being

$$\epsilon_{Bc} = 0.30\ \mathrm{Ar}^{0.04} \quad (2 < \mathrm{Ar} < 2 \times 10^6) \quad [9]$$

The minimum transport velocity, also called the type A choking velocity and defined as the point where the uniform suspension collapses, causing particles to begin to accumulate at the bottom of the transport line with reducing the gas velocity (Bi *et al.* 1993), is predicted by

$$V_{CA} = U_{sc} + \frac{G_s \epsilon_{CA}}{\rho_p (1 - \epsilon_{CA})} \quad [10]$$

The bed voidage at this transition point, ϵ_{CA}, ranges from 0.96 to 0.99, depending on particle properties (Bi *et al.* 1995). For group A particles, ϵ_{CA} is around 0.96, while for group B and group D particles, ϵ_{CA} is around 0.99.

The minimum slugging velocity in systems that exhibit slugging can be estimated by

$$V_{ms} = U_{ms} + \frac{G_s \epsilon_{ms}}{\rho_p (1 - \epsilon_{ms})} \quad [11]$$

where U_{ms} can be estimated by an equation due to Stewart & Davidson (1967)

$$U_{ms} = U_{mf} + 0.07\sqrt{gD} \quad [12]$$

ϵ_{ms} is estimated to be about 0.55 if the slug volume fraction is taken to be 1/6 (Stewart & Davidson 1967). In columns of large diameter or for very small particles, a slug flow regime does not exist. The region between V_c and V_{mb} then corresponds entirely to the bubbly flow regime.

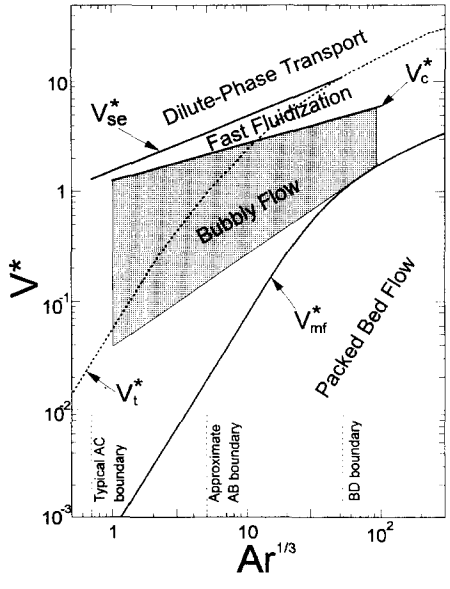

Figure 4. Idealized flow regime map for gas–solids upward transport. Heavy lines indicate transition velocities The shaded region bounded by thin lines portrays the typical operating range for bubbly flow with solids flux maintained constant.

Based on the above considerations, a flow regime diagram, figure 4, similar to figure 2, can be produced with Ar as the abscissa axis and V^*, defined as

$$V^* = \left[\frac{\rho_G^2}{g\mu_G(\rho_p - \rho_G)}\right]^{1/3}\left[V - \frac{G_s\epsilon}{\rho_p(1-\epsilon)}\right] \quad [13]$$

as the ordinate. Since both the minimum slugging velocity, V_{ms}, and the velocity corresponding to the minimum pressure drop, V_{mp}, depend on column diameter, they cannot be included in this diagram. For a batch operated fluidized bed with given particles, the flow pattern is determined by the superficial gas velocity only. For $G_s = 0$, figure 4 becomes the same as figure 2 with $V^* = U^*$. Figure 4 can thus be considered as a generalized flow regime diagram. In a solids transport system with given particles, the flow pattern depends on both the superficial gas velocity and the solids circulation rate. To determine the flow pattern under given operating conditions, both Ar and V^* need to be calculated and then located on figure 4 to determine the flow pattern.

The pneumatic transport regime has been extensively studied (Marcus *et al.* 1990), while relatively few studies have been reported on dense-phase transport (Konrad 1986), possibly because it is relatively difficult to maintain dense-phase flow under stable operation. Unlike pneumatic transport above the type A choking velocity where particles are fully suspended in the gas, particles in dense-phase transport are in contact and travel like a piston, requiring a relatively high pressure drop and a high feed rate of particles. When the gas blower is unable to provide sufficient pressure head or solids cannot be fed to the riser at the required rate, stable operation of dense-phase flow becomes impossible due to type B choking (Bi *et al.* 1993). In some cases, even though sufficient blower pressure and solids feeding are provided, it is impossible to achieve dense-phase transport due to severe slugging, i.e. due to type C "classical choking" (Bi *et al.* 1993).

The map in figure 4 is idealized with no equipment-related restrictions. In circulating fluidized beds and transport risers, dense-phase operation below V_c is difficult to realize due to limitations in gas blowers and solids feed devices. In real systems, stable operation of dense-phase transport may terminate at the type B choking velocity and/or type C choking velocity (Bi *et al.* 1993). This is clearly demonstrated in figure 5 where three possible flow transition routes with decreasing superficial gas velocity at a fixed solids circulation rate are included. The reverse transition route in figure 3 can be realized only in systems with no equipment-related restrictions and with no classical choking occurring.

A circulating fluidized bed is generally operated in the region between the type A and the type B or C choking velocities and with the gas velocity close to the minimum pressure gradient point, V_{mp}. It can be considered to cover both the turbulent flow and the core–annular dilute flow regimes, as indicated in figure 5. A fast fluidization regime is usually characterized by a concentration profile consisting of a dense bottom region and dilute top region. Such a combination is similar to what is found in the turbulent flow regime bounded in figure 5 by the type B or C choking velocities and the type A choking velocity. In most cases, it is impossible to operate a circulating fluidized bed under dense-phase transport conditions because insufficient

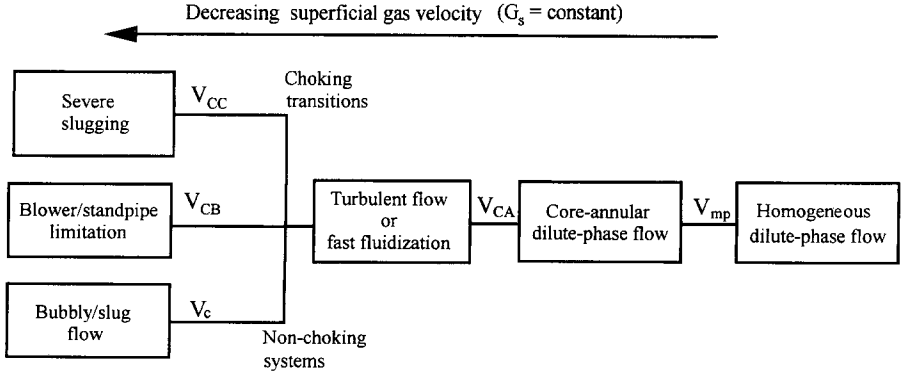

Figure 5. Flow chart showing regime transitions in circulating fluidized beds and transport risers with decreasing gas flow.

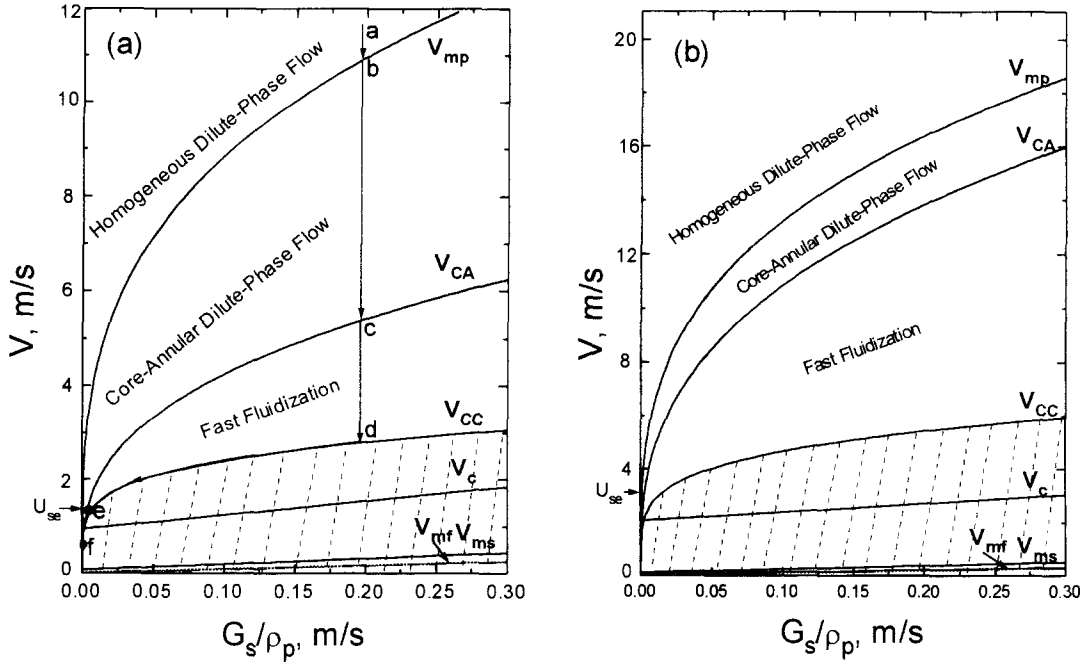

Figure 6. Practical flow regime maps for gas–solids upward transport in the presence of restrictions for (a) group A FCC particles, $d_p = 60\ \mu m$, $\rho_p = 1500\ kg/m^3$, $D = 0.15\ m$; (b) group B sand particles, $d_p = 200\ \mu m$, $\rho_p = 2600\ kg/m^3$, $D = 0.15\ m$. The shaded regions indicate zones when practical operation is very difficult if not impossible.

solids can be provided from the standpipe owing to pressure imbalance between the riser and downcomer.

Figure 6(a) and (b) shows modified maps for typical circulating fluidized beds and transport riser operation with G_s/ρ_p as the abscissa and V/U_t as the ordinate. In this map the classical choking velocity is obtained from the equation of Yousfi & Gau (1974)

$$V_{CC}/\sqrt{gd_p} = 32\ Re_t^{-0.06}(G_s/\rho_G V_{CC})^{0.28} \quad [14]$$

while V_{CA} is estimated using the equation of Bi & Fan (1991)

$$V_{CA}/\sqrt{gd_p} = 21.6\ Ar^{0.105}(G_s/\rho_G V_{CA})^{0.542} \quad [15]$$

The minimum pressure-drop point denotes the transition from homogeneous dilute flow to core–annular dilute flow conditions (Leung 1980, Klinzing 1981). Accurate quantitative determination of this transition is made difficult by the uncertainty of the solid friction factor and solid acceleration term in the momentum balance equations. As a first approximation, the Bi & Fan (1991) correlation.

$$V_{mp} = 10.1(gd_p)^{0.347}(G_s/\rho_G)^{0.310}\left(\frac{d_p}{D}\right)^{-0.139} Ar^{-0.021} \quad (16)$$

may be used to estimate this transition.

It is seen in figure 6(a) that the fast fluidization regime for FCC is virtually non-existent for superficial gas velocities less than U_{se}, As a result, a fast fluidization regime can only be realized at gas velocities greater than U_{se}. Comparing figure 6(a) for group A particles and figure 6(b) for group B particles, it is seen that the core–annular dilute-phase flow regime becomes narrower for larger particles. A core–annular dilute-flow regime probably does not exist for group D particles, because the suspension collapses, giving a dense region at the bottom, as soon as a core–annular structure is established, due to the formation of particle streamers near the wall. This is consistent with the finding (Bi *et al.* 1995) that U_{se} is almost the same as U_t for large group D particles.

Table 1. Key characteristics of the turbulent fluidization, fast fluidization and dilute phase transport regimes

Characteristic	Turbulent fluidization	Fast fluidization	Core–annular dilute transport	Homogeneous dilute transport
Gas velocity range	$U_c < U < U_{se}$	$U_{se} < U < V_{CA}$ or $V_{Ch} < U$	$V_{CA} < U < V_{mp}$	$U < V_{mp}$
Solids flux range†	$G_s \leqslant G_{s,CA}$	$G_s > G_{s,CA}$	$G_s < G_{s,CA}$	$G_s \ll G_{s,CA}$
Overall voidage	$\epsilon = 0.6$–0.8	$\epsilon = 0.8$–0.95	$\epsilon = 0.95$–0.99	$\epsilon > 0.99$
Axial particle gradients	High	High	Low	None
Radial voidage gradient	Moderate	High	High	Low
Gas–solids relative velocity	Low	High	Low	$\approx U_t$
Particle backmixing	High	High	Low	None

†$G_{s,CA}$ = saturation carrying capacity of the fluid (kg/m^{2}s)

Table 1 summarizes key characteristics of different high velocity fluidization regimes. A typical transition process with decreasing gas velocity and constant G_s is indicated in figure 6(a) by line a–b–c–d–e–f. At a constant solids circulation rate, the transport line is operated in the homogeneous dilute flow regime without lateral solids segregation at gas velocities higher than that corresponding to point b. Particle streamers do not form near the column wall. Particle streamers start to form due to the particle–wall interaction when the gas velocity is reduced to point b, and the core–annular structure develops as the gas velocity is reduced from point b to point c. The axially uniform suspension collapses at point c with a collapsed dense phase forming in the bottom and a core–annular flow persisting in the upper section. The transport line becomes unstable when the gas velocity is decreased to point d, due to either type B or type C choking. The solids circulation rate can then no longer be held constant when the superficial gas velocity is further decreased below point d. As a result, the solids circulation rate drops along line d–e. Eventually, the solids circulation rate reaches $G_{s,CA}$, the saturated carrying capacity of the saturated entrainment rate. A further decrease in gas velocity causes the operation to travel along the entrainment curve (i.e. line e–f) because particles can only be entrained by the gas, as in a conventional fluidized bed.

4. CONCLUSION

Flow regime maps are presented for gas–solids fluidized beds and gas–solids upward transport lines. For conventional gas–solids fluidization operation (i.e. $G_s \approx 0$), the flow regimes include the fixed bed, bubbling bed, slugging bed and turbulent bed regimes. Beyond U_{se} particles are significantly entrained from the fluidized bed, and it is possible to operate under steady conditions with very low G_s and appreciable solids concentrations. For gas–solids vertical transport operation, the solids flux, G_s, must be incorporated in the flow regime diagrams. The flow regimes then include dilute-phase transport, fast fluidization or turbulent flow, slug/bubbly flow, bubble-free dense-phase fluidization and packed bed flow. In practical operation of circulating fluidized beds and transport risers, operation below the turbulent flow regime is usually impossible due to equipment restrictions. Practical flow regime maps are then proposed with V plotted against G_s/ρ_p and with the flow regimes including homogeneous dilute flow without appreciable lateral and axial gradients of voidage, core–annular dilute phase flow where there are appreciable lateral gradients but small axial gradients, and fast fluidization or turbulent flow where both lateral and axial gradients are significant.

The flow regimes in conventional fluidized beds and dilute-phase transport have been studied quite extensively and are relatively clear. Transitions in dense-phase transport lines require further study using transport lines capable of being operated at high solids fluxes and densities.

REFERENCES

Bi, H. T. & Fan, L.-S. 1991 Regime transitions in gas–solid circulating fluidized beds. *AIChE Annual Meeting*, Los Angeles, 17–22 November.

Bi, H. T. & Grace, J. R. 1994 Transition from bubbling to turbulent fluidization. *AIChE Annual Meeting*, San Francisco, 13–18 November.

Bi, H. T. & Grace, J. R. 1995 Effects of measurement methods on velocities used to demarcate the transition to turbulent fluidization. *Chem. Engng J.* **57**, 261–271.

Bi, H. T., Grace, J. R. & Zhu, J. X. 1993 On types of choking in pneumatic systems. *Int. J. Multiphase Flow* **19,** 1077–1092.

Bi, H. T., Grace, J. R. & Zhu, J. X. 1995 Regime transitions affecting gas–solids suspensions and fluidized beds. *Chem. Engng Res. Des.* **73,** 154–161.

Geldart, D. & Abrahamsen, A. R. 1978 Homogeneous fluidization of fine powders using various gases and pressures. *Powder Technol.* **19,** 133–136.

Grace, J. R. 1982 Fluidized bed hydrodynamics. In *Handbook of Multiphase Flow* (Edited by Hetsroni, G.), Chap. 8.1. Hemisphere, Washington, DC.

Grace, J. R. 1986 Contacting modes and behaviour classification of gas–solid and other two-phase suspensions. *Can. J. Chem. Engng* **64,** 353–363.

Hirama, T., Takeuchi, T & Chiba, T. 1992 Regime classification of macroscopic gas–solid flow in a circulating fluidized-bed riser. *Powder Technol.* **70,** 215–222.

Klinzing, G. E. 1981 *Gas–Solid Transport.* McGraw–Hill, New York.

Konrad, K. 1986 Dense-phase pneumatic conveying: a review. *Powder Technol.* **49,** 1–35.

Leung, L. S. 1980 Vertical pneumatic conveying: a flow regime diagram and a review of choking versus non-choking systems. *Powder Technol.* **25,** 185–190.

Marcus, R. D., Leung, L. S., Klinzing, G. E. & Rizk, F. 1990 Flow regimes in vertical and horizontal conveying. In *Pneumatic Conveying of Solids*, Chap. 5, pp. 159–191. Chapman & Hall, New York.

Reh, L. 1971 Fluid bed processing. *Chem Engng Prog.* **67,** 58–63.

Rhodes, M. J. 1989 The upward flow of gas/solid suspensions. Part 2: a practical quantitative flow regime diagram for the upward flow of gas/solid suspensions. *Chem. Engng Res. Des.* **67,** 30–37.

Squires, A. M., Kwauk, M. & Avidan, A. A. 1985 Fluid beds: at last, challenging two entrenched practices. *Science* **230,** 1329–1337.

Stewart, P. S. B. & Davidson, J. F. 1967 Slug flow in fluidized beds. *Powder Technol.* **1,** 61–80.

Takeuchi, H., Hirama, L., Chiba, T., Biswas, J. & Leung, L. S. 1986 A quantitative regime diagram for fast fluidization. *Powder Technol.* **47,** 195–199.

Wen, C. Y. & Yu Y. H. 1966 A generalized method for predicting the minimum fluidization velocity. *AIChE Jl* **12,** 610–612.

Yerushalmi, J., Turner, D. H. & Squires, A. M. 1976 The fast fluidized bed. *Ind. Engng Chem. Proc. Des. Dev.* **15,** 47–51.

Yerushalmi, J., Cankurt, N. T., Geldart, D. & Liss, B. 1978 Flow regimes in vertical gas–solid contact systems. *AIChE Symp. Ser.* **174**(176), 1–12.

Yousfi, Y. & Gau, G. 1974 Aerodynamique de l'écoulement vertical de suspensions concentrées gaz–solides—I. Régimes d'écoulement et stabilité aerodynamique. *Chem. Engng Sci.* **29,** 1939–1946.

Zenz, F. A. 1949 Two-phase fluidized-solid flow. *Ind. Engng Chem.* **41,** 2801–2806.